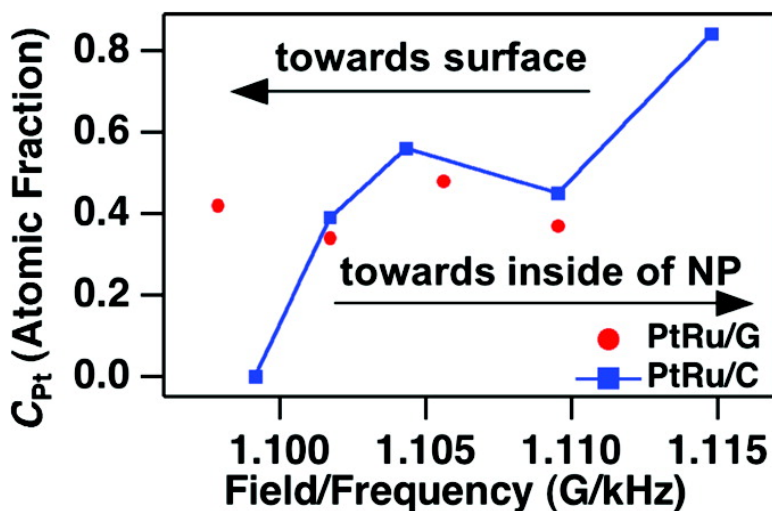


## Probing Spatially-Resolved Pt Distribution in PtRu Nanoparticles with Pt EC-NMR

Aaron L. Danberry, Bingchen Du, In-Su Park, Yung-Eun Sung, and Tong

*J. Am. Chem. Soc.*, 2007, 129 (45), 13806-13807 • DOI: 10.1021/ja076048v • Publication Date (Web): 19 October 2007

Downloaded from <http://pubs.acs.org> on February 14, 2009



### More About This Article

Additional resources and features associated with this article are available within the HTML version:

- Supporting Information
- Links to the 3 articles that cite this article, as of the time of this article download
- Access to high resolution figures
- Links to articles and content related to this article
- Copyright permission to reproduce figures and/or text from this article

[View the Full Text HTML](#)

## Probing Spatially-Resolved Pt Distribution in PtRu Nanoparticles with $^{195}\text{Pt}$ EC-NMR

Aaron L. Danberry,<sup>†</sup> Bingchen Du,<sup>†</sup> In-Su Park,<sup>‡</sup> Yung-Eun Sung,<sup>‡</sup> and YuYe Tong<sup>\*†</sup>

Department of Chemistry, Georgetown University, 37th and O Streets NW, Washington, District of Columbia 20057, and School of Chemical & Biological Engineering, Seoul National University, Seoul 151-744, South Korea

Received August 11, 2007; E-mail: yyt@georgetown.edu

Pt-based alloy metal nanoparticles (NPs) have long been widely used in petroleum and automobile industries as work-horse catalysts.<sup>1</sup> They also hold great promises for developing economically viable clean energy sources (fuel cells) for practical applications such as land-based transportation.<sup>2</sup> While much has been intensively researched, further mechanistic understanding required for an eventual rational design of better catalysts is often hindered by lack of detailed and reliable knowledge of the *local* distribution of the alloying elements which is key to understand both the overall electronic and locally specific surface-bonding properties that are ultimately responsible for the catalytic actions of the NPs.<sup>1</sup> Access to such information experimentally, however, is still of a challenging prospect. The current method of choice is probably the X-ray based spectroscopic techniques such as XPS and EXAFS. But these techniques can only provide average distribution of the alloying elements. In this Communication we report a (semi-) spatially resolved quantitative analysis of the local distribution of Pt in carbon-supported PtRu NPs using the RKKY (Ruderman–Kittel–Kasuya–Yosida) *J* coupling<sup>3</sup> measurements by in situ  $^{195}\text{Pt}$  electrochemical NMR (EC-NMR).<sup>4</sup>

It has been well argued in the classic papers of Froidevaux and Weger<sup>5</sup> and of Slichter and companies<sup>6</sup> that the *J*-coupling generated modulation of the Hahn spin echo amplitude (i.e., slow beats) can be expressed by eq 1, provided that the resonant frequency difference between the nearest neighboring nuclear spins is much larger than the *J*-coupling constant *J*:

$$S(\tau)/S_0 = \exp(-2\tau/T_2) \{ P_0 + \exp[-(\tau/T_2)^2] \sum_{n=1}^{12} P_n \cos^n(J\tau) \} \quad (1)$$

where  $\tau$  is the time interval between the two pulses in the spin-echo sequence,  $T_2$  is the nuclear spin-spin relaxation time,  $T_{2f}$  accounts for a Gaussian-type spread in *J* owing to the inevitable environmental heterogeneity, and  $P_n$  is the probability of having *n* nearest neighboring nuclear spins and therefore a function of their concentration. So, by determining the  $P_n$ , one can access concentration of the unclear spin under observation. Indeed, such an idea has been briefly explored by Slichter and companies.<sup>7</sup>

Two PtRu alloy NP samples with nominal atomic ratio of 1:1 have been investigated here: PtRu NPs supported on graphite nanofibers (abbreviated as G) and on carbon nanofibers (abbreviated as C) with an overall metal loading of 60% (wt).<sup>8</sup> The transmission electron microscope (TEM) determined average particle size was 4.1 nm for the former and 3.9 nm for the latter (inset in Figure 1). For  $^{195}\text{Pt}$  NMR measurements, about 80 mg of the PtRu NPs was loaded into a 5 mm (*d*)  $\times$  25 mm (*l*) NMR glass sample cell which was then attached to a three-electrode electrochemical (EC) setup as a working electrode compartment. Electrical contact was achieved by burying a gold wire into the sedimented PtRu NPs. The

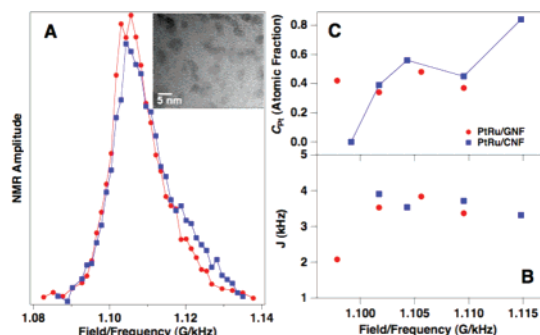


**Figure 1.** (A) The point-by-point, area-normalized  $^{195}\text{Pt}$  NMR spectra of the PtRu/G and PtRu/C NPs at 80 K. The inset is a TEM image of the PtRu/G. (B) The *J* coupling constants deduced by fitting the slow-beat curves to eq 1. (C) The Pt atomic fraction deduced by analyzing the  $P_0$  values using eq 2.

supporting electrolyte was 0.5 M  $\text{HClO}_4$  and reference and counter electrodes were a commercial Ag/AgCl (3M) electrode and a 3 mm Pt electrode (Bianalytical), respectively. The sample was first EC cleaned by holding potential at 0.2 V (vs Ag/AgCl) until current decayed down to and stabilized at about 60  $\mu\text{A}$  (which usually took 48–72 h). During the cleaning process, the cell was periodically blanketed by ultrapure Ar. After the EC cleaning, the NMR sample cell filled with the supporting electrolyte was detached from the EC setup under Ar blanketing, sealed immediately with a one-to-one grounded glass stopper, inserted into the NMR probe, and then loaded down to the precooled (80 K) cryostat. After the NMR measurements, the sample cell was reattached to the EC setup and the open circuit potential was checked. In all cases, the open potential was within 10 mV difference before and after the NMR measurements. All  $^{195}\text{Pt}$  NMR measurements reported here were carried out at 80 K on a “home-assembled” spectrometer equipped with an active-shielded 9.395 T widebore superconducting magnet, an Oxford SpectrostatCF cryostat (Oxford Instruments, U.K.), an AMT (Lancaster, PA) 1 kw power amplifier, a Tecmag (Houston, TX) Appollo data acquisition system, and a home-built single-channel solenoid probe. The spectra (Figure 1A) were obtained with the conventional “ $\pi/2$ – $\tau$ – $\pi$ – $\tau$ –echo” Hahn spin-echo sequence point-by-point by varying the frequency between ca. 82–87 MHz. The values of  $\pi/2$  pulse length and  $\tau$  were 3  $\mu\text{s}$  (corresponding to a  $B_1$  of 90 G) and 25  $\mu\text{s}$ , respectively. The slow beats were measured by varying  $\tau$  in the spin-echo sequence.

A uniqueness of  $^{195}\text{Pt}$  NMR of Pt NPs is that within a certain spectral range a given spectral frequency (*f*) can be quantitatively related to a given geometric position of atoms (*r*) via the so-called layer model.<sup>9–11</sup> Qualitatively, this can be stated as: The surface atoms resonate at the low-field end (centered at 1.100 G/kHz) and the bulklike atoms resonate at the high-field end (centered at 1.138 G/kHz). As the *r* becomes farther away from the surface and deeper into the NPs, the *f* gradually shifts upfield toward the bulk position. Thus, an *f*–*r* correlation can be established which offers a unique

<sup>†</sup> Georgetown University.

<sup>‡</sup> Seoul National University.

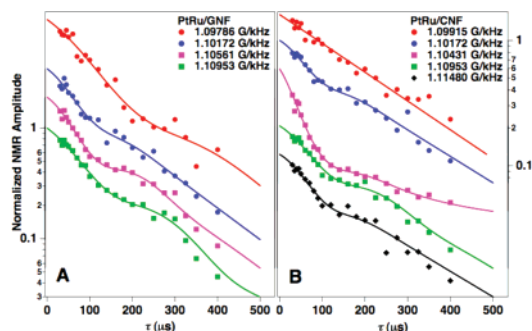


**Figure 2.** The slow beats measured at different spectral positions for (A) PtRu/G and (B) PtRu/C. The solid curves are the fits to eq 1.

way to access spatially resolved information<sup>10,11</sup>. Although no quantitative layer-model analysis has been done yet for Pt-based alloy NPs, available data on PtPd<sup>12</sup> and PtRh<sup>7</sup> alloy NPs, however, indicate strongly that the qualitative statement of the  $f-r$  correlation still holds. We assume that it is also applicable to PtRu NPs studied here (a preliminary analysis of the Fermi level local density of states ( $E_F$ -LDOS) based on spin-lattice  $T_1$  relaxation measurements indeed supports this assumption). Figure 1A shows the point-by-point, area-normalized <sup>195</sup>Pt NMR spectra of the PtRu/G (red dots) and PtRu/C (blue squares) NPs, and the inset is a representative TEM image of the former. No PtO<sub>x</sub> signal at 1.089 G/kHz was observed, ensuring the effectiveness of the EC cleaning. The overall line shape of the spectra is similar to each other and to that of a PtRu black sample published previously,<sup>13</sup> but the lack of distinguishable surface versus bulklike signals is in contrast to those observed in the pure Pt NPs of similar size (vide supra). However, the spectra were broad enough to satisfy the criterion for observing the slow beats.<sup>5,6</sup>

Figure 2 presents the across-the-spectrum slow beats data. The solid curves are the fits to eq 1 with  $T_2$ ,  $T_{2j}$ ,  $J$ ,  $P_0$ ,  $P_1$  as fitting parameters and  $P_2 = 1 - P_0 - P_1$ ; all other  $P_n$  could be neglected (see Tables S2 and S3 in Supporting Information). The  $J$  constants so obtained are shown in Figure 1B, which to a large degree are invariant across the spectrum for both samples and very close to those obtained on pure Pt NPs. Additionally, these  $J$  values are in good agreement with those calculated from the s-like  $E_F$ -LDOS<sup>10</sup> which was determined by the independent  $T_1$  measurements, validating the soundness of the fits. On the other hand, the  $P_0$  ( $P_1$ ) values for the PtRu/C show a strong variation across the spectrum. This is qualitatively evident by simply inspecting the slow beat curves in Figure 2B of which the most obvious is the lack of slow beat at 1.09915 G/kHz. It is highly unlikely that the Knight shift gradient at 1.09786 G/kHz was significantly different from that at 1.09915 G/kHz. Additionally, a  $B_1$  of 90 G was strong enough to reach the asymptote<sup>7</sup> for the slow beats. Therefore, the absence of the slow beat at 1.09915 G/kHz for the PtRu/C suggests that the Pt atoms resonating there were dominantly coordinated with Ru atoms. To extract quantitatively the Pt concentration from the  $P_0$  values, we adapted the model developed by Slichter and companies<sup>6</sup> that enables analytical expressions of  $P_n$  to be developed for situations of large Knight shift gradient, that is,  $\delta = \omega_1/(a\omega_0|\nabla K|) \ll 1$ , where  $a$  is the distance between nearest neighbors,  $\omega_1$  and  $\omega_0$  are the Larmor frequencies under the  $B_1$  and the external static field, and  $\nabla K$  is the local Knight shift gradient. Briefly,  $P_n$  can be expressed as

$$P_n = \sum_{i=n}^{12} A_{ni} Q_n \quad (2)$$

where  $Q_n$  is the probability of having  $n$  nearest neighbors whose

spins can be flipped by the  $B_1$  and  $A_{ni}$  is the probability of  $i$  out of the  $n$  nearest neighbors being the <sup>195</sup>Pt isotope (nature abundance is 0.337). While  $A_{ni}$  is a function of the Pt atomic fraction  $C_{Pt}$  ( $=1$  for bulk Pt),  $Q_n$  is a function of the  $\delta$ , and the maximum value of  $n$  for the model used here is 6 (see the original paper<sup>6</sup> for detailed discussions). For simplicity, we also assume that  $\delta$  is a constant across the spectrum and take an ad hoc value of 0.1 (estimated from the values obtained on pure Pt NPs at 1.1145 G/kHz<sup>10</sup> and 1.117 G/kHz<sup>6</sup>, respectively, where similar values of  $\delta$  are expected). The  $C_{Pt}$  was then deduced from  $P_0$  by solving eq 2 under the constrain of  $\sum P_n = 1$ . The results so obtained are presented in Figure 1C (also in Tables S2 and S3 in the Supporting Information). Using the  $C_{Pt}$  values so obtained and  $\delta = 0.1$ , the corresponding  $P_1$  values were calculated using eq 2. Overall, these calculated values were in excellent agreement with those determined by the slow-beat fits, substantiating further the internal consistency of the analysis. Most remarkably, the results show that PtRu/G had a rather homogeneous distribution of Pt but not so for PtRu/C whose data indicate that there was Pt segregation at the core (high-field end) and depletion at the surface (low-field end) of the NPs and a rather homogeneous distribution in-between. Notice that the Pt segregation at the core is consistent with the observation that the spectral amplitude above 1.115 G/kHz for PtRu/C was higher than that for PtRu/G (Figure 1A). Also, the NMR-amplitude-weighted average  $C_{Pt}$  values are 0.42 and 0.47 for PtRu/G and PtRu/C, respectively, very close to the nominal value of 0.5.

In summary, we reported the first (semi-) spatially resolved analysis of the local Pt distribution within PtRu NPs utilizing the unique  $f-r$  correlation offered by <sup>195</sup>Pt NMR of Pt-based NPs. This approach is applicable to other Pt-based alloy NPs, and a broader availability of such spatially resolved elemental composition in NPs will have profound ramifications for achieving a fundamental understanding of the catalytic actions of a given Pt-based alloy NP catalyst.

**Acknowledgment.** A.L.D. is a NSF REU summer student from Minnesota State University at Mankato. I.S.P. and Y.E.S. thank the Ministry of Science and Technology, the KOSEF through the Research Center for Energy Conversion and Storage, and KRF (Grant KRF-2004-005-D00064) for financial support. B.D. and Y.Y.T. acknowledge the financial support by NSF (Grant CHE-0456848) and DOE (Grant DE-FG02-07ER15895).

**Supporting Information Available:** More information on NP synthesis and on data analysis. This material is available free of charge via the Internet at <http://pubs.acs.org>.

## References

- (1) Ponec, V.; Bond, G. C. *Catalysis by Metal and Alloys*; Elsevier: Amsterdam, Netherlands, 1995.
- (2) Wee, J.-H.; Lee, K.-Y. *J. Power Source* **2006**, *157*, 128–135.
- (3) Ruderman, M. A.; Kittel, C. *Phys. Rev.* **1954**, *96*, 99–102.
- (4) Tong, Y. Y.; Wieckowski, A.; Oldfield, E. *J. Phys. Chem. B* **2002**, *106*, 2434–2446.
- (5) Froidevaux, C.; Weger, M. *Phys. Rev. Lett.* **1964**, *12*, 123–125.
- (6) Stokes, H. T.; Rhodes, H. E.; Wang, P.-K.; Slichter, C. P.; Sinfelt, J. H. *Phys. Rev. B* **1982**, *26*, 3575–3581.
- (7) Wang, Z.; Ansermet, J.-P.; Slichter, C. P.; Sinfelt, J. H. *J. Chem. Soc. Faraday Trans.* **1988**, *84*, 3785–3802.
- (8) Park, I.-S.; Park, K.-W.; Choi, J.-H.; Park, C. R.; Sung, Y.-E. *Carbon* **2007**, *45*, 28–33 (see also Supporting Information for more details).
- (9) Bucher, J. P.; Buttet, J.; van der Klink, J. J.; Graetzel, M. *Surf. Sci.* **1989**, *214*, 347–357.
- (10) Tong, Y. Y.; Babu, P. K.; Wieckowski, A.; Oldfield, E. *Chem. Phys. Lett.* **2002**, *361*, 183–188.
- (11) Tong, Y. Y.; Zelakiewicz, B. S.; Dy, B. M.; Pogozelski, A. R. *Chem. Phys. Lett.* **2005**, *406*, 137–142.
- (12) Tong, Y. Y.; Yonezawa, T.; Toshima, N.; Klink, J. J. v. d. *J. Phys. Chem.* **1996**, *100*, 730–733.
- (13) Babu, P. K.; Kim, H. S.; Oldfield, E.; Wieckowski, A. *J. Phys. Chem. B* **2003**, *107*, 7595–7600.

JA076048V